Available online at www.sciencedirect.com

ScienceDirect

Ceramics International 39 (2013) 8877–8883

CERAMICS INTERNATIONAL

www.elsevier.com/locate/ceramint

# High temperature mechanical properties of $Al_2O_3$/TiC micro–nano-composite ceramic tool materials

Zengbin Yin[a,b], Chuanzhen Huang[a,b,*], Bin Zou[a,b], Hanlian Liu[a,b], Hongtao Zhu[a,b], Jun Wang[a,b]

[a]*Centre for Advanced Jet Engineering Technologies (CaJET), School of Mechanical Engineering, Shandong University, Jinan 250061, PR China*

[b]*Key Laboratory of High-efficiency and Clean Mechanical Manufacture (Shandong University), Ministry of Education, PR China*

Received 26 February 2013; received in revised form 10 April 2013; accepted 24 April 2013
Available online 1 May 2013

**Abstract**

A type of $Al_2O_3$-based composite ceramic tool material simultaneously reinforced with micro-scale and nano-scale TiC particles was fabricated by the hot-pressing technology with different contents of cobalt additive. The effects of cobalt on the ambient temperature mechanical properties and high temperature flexural strength were investigated. The flexural strength and fracture toughness of the composite with 3 vol% cobalt as a function of temperature were investigated. Cobalt greatly enhanced the ambient temperature flexural strength and fracture toughness, while further increasing the content of cobalt led to a dramatic strength degradation, especially at high temperature. The flexural strength of the composite containing 3 vol% cobalt decreased as the temperature increased from 20 to 1200 °C, and the fracture toughness decreased as a function of the temperature up to 1000 °C but increased at 1200 °C. The degradation of high temperature flexural strength was ascribed to the change of the fracture mode, the grain and grain boundary oxidation, the decrease of elastic modulus and the grain boundary sliding.


*Keywords:* B. Composites; C. Fracture; C. Strength; E. Cutting tools

## 1. Introduction

$Al_2O_3$-based ceramic tool materials have great advantages in the field of high-speed machining compared to the traditional high-speed steel and cemented carbide cutting tools, due to the high hardness, excellent wear and corrosion resistance, as well as the low affinity with metal. They can also machine hardened steel, nickel based alloys and other difficult-to-cut materials, therefore, the ceramic tool materials are considered as one of the most promising and competitive tool materials [1]. However, the brittleness and poor damage tolerance have limited the wide application of alumina ceramics. Up to now, much effort has been made to improve the strength and toughness of ceramic materials. Several useful methods, such as dispersion of multi-scale particles in the brittle matrix [2–6], fiber or whisker reinforced composites [7], phase transformation toughening as revealed by zirconia [8,9] and incorporation of ductile phase into the brittle ceramic matrix [10] have been proposed. In the previous work we have successfully fabricated the $Al_2O_3$/TiC micro–nano-composite ceramic tool material containing 6 vol% nano-scale TiC particles and 35 vol% micro-scale TiC particles, which was sintered under a pressure of 32 MPa at 1650 °C in a vacuum for 20 min. Its optimum ambient temperature mechanical properties were a flexural strength of 916 MPa, a fracture toughness of 8.3 MPa $m^{1/2}$ and a Vickers hardness of 18 GPa [11].

When machining the difficult-to-cut materials, the cutting temperature is usually high, e.g., when cutting Inconel 718 with ceramic cutting tools, the average cutting temperature on the tool rake face was 800–850 °C at the cutting speed of 101 m/min, and the temperature could reach up to 1088 °C as the cutting speed increased to 175 m/min [12]. The deformation and strength change of ceramics with the temperature were the primary cause of tool wear, breakage and failure [13]. Thus, the high temperature mechanical properties

*Corresponding author at: Centre for Advanced Jet Engineering Technologies (CaJET), School of Mechanical Engineering, Shandong University, Jinan 250061, PR China. Tel./fax: +86 531 88396913.
*E-mail address:* chuanzhenh@sdu.edu.cn (C. Huang).

0272-8842/$ - see front matter © 2013 Elsevier Ltd and Techna Group S.r.l. All rights reserved.
http://dx.doi.org/10.1016/j.ceramint.2013.04.081

of ceramic cutting tool material are very important to determine whether it suits to be used in the high speed machining. Additionally, studies on the high temperature mechanical properties of the tool material are useful to analyze the causes of tool failure in the cutting process. However, very few reports on the high temperature mechanical properties of ceramic cutting tool materials are noted. In this paper, the flexural strength and fracture toughness of the $Al_2O_3$/TiC micro–nano-composites with different contents of cobalt at room and high temperature were investigated.

## 2. Experimental procedures

### 2.1. Materials preparation

The starting materials were α-$Al_2O_3$ powder with an average particle size of 0.5 μm (purity: 99.99%, Shanghai, China), nano-scale TiC with an average particle size of 40 nm (purity: 99.9%, Shanghai, China), micro-scale TiC with an average particle size of 0.5 μm (purity: 99%, Hefei, China) and Co with an average particle size of 2 μm (purity: 99.9%, Shanghai, China). Four kinds of composites containing different contents of cobalt were fabricated and tested as shown in Table 1. The nano-scale TiC powder was prepared in a suspension using alcohol as the dispersing medium, and the dispersant PEG (polyethylene glycol, Shanghai, China) was added after ultrasonic dispersion (with a SB5200 ultrasonic instrument and a D-7401-III motor stirrer, China) for 10 min. The suspension was dispersed ultrasonically for 20 min after a pH of 9.0 (with a PHS-25 digimatic pH-meter, China) was attained by the addition of $NH_3 \cdot H_2O$. After that, the nano-scale TiC particle suspensions were mixed with $Al_2O_3$, micro-scale TiC and Co. The mixed slurries were ball-milled for 48 h, and then dried in a vacuum dry-type evaporator (Moder ZK-82A, China). After that, the ball-milled powders were sieved through a 200-mesh sieve for further use. The dried powders were placed into a graphite die and hot-pressed with an applied pressure of 32 MPa at 1650 °C with the holding time of 20 min in a vacuum in a sintering furnace.

### 2.2. Mechanical properties tests

The sintered compacts were cut, ground and polished into samples with the size of 3 mm × 4 mm × 38 mm for the flexural strength test and 4 mm × 2 mm × 38 mm for the fracture toughness test. Both the flexural strength and the fracture toughness were tested at 20, 800, 1000 and 1200 °C in air. The flexural strength was tested using the three-point bending tester (INSTRON 8801, Britain) with a span of 30 mm and a loading velocity of 0.5 mm/min. The fracture toughness was measured using the single-edge-notched-beam (SENB) method on the three-point bending tester (INSTRON 8801, Britain) with a span of 30 mm and a loading velocity of 0.05 mm/min. Notches were incised in the middle of the samples along the height using a circular saw with a width of 0.2 mm to the depth of about 2 mm. The samples were soaked at the testing temperature for 15 min to reach a thermal equilibrium. The Vickers hardness was measured on the polished surface using a Vickers diamond pyramid indenter (Model 120, China) with a load of 196 N and a loading holding time of 15 s. The microstructure of the composite was observed by scanning electron microscopy (SEM, SUPRA-55, ZEISS, Germany). Phase identification was carried out by X-ray diffraction analysis (XRD, RAX-10A X, Hitachi, Japan) with Cu Kα radiation.

Table 1
Composition (vol%) of different composites.

| Composites | $Al_2O_3$ (0.5 μm) | TiC (40 nm) | TiC (0.5 μm) | Co (2 μm) |
|---|---|---|---|---|
| ATC0 | 59 | 6 | 35 | 0 |
| ATC3 | 56 | 6 | 35 | 3 |
| ATC5 | 54 | 6 | 35 | 5 |
| ATC8 | 51 | 6 | 35 | 8 |

## 3. Results and discussion

### 3.1. Effects of cobalt content on mechanical properties and microstructure

The ambient temperature mechanical properties and high temperature flexural strength versus the cobalt content are shown in Fig. 1.

At ambient temperature, it can be seen that the flexural strength and hardness increased with the content of cobalt increasing from 0 to 3 vol%, but decreased with the further increase of cobalt content. The fracture toughness increased straightly with the increase of cobalt content. SEM micrographs of the fractured surfaces of samples tested at ambient temperature are shown in Fig. 2. It can be seen that the microstructure of ATC0 was not homogeneous with large grains. There were plenty of pores distributed not only at grain boundaries but also in grains, which were disadvantageous to the flexural strength. The fracture mode of ATC0 was mainly intergranular fracture, indicating a poor interfacial bonding strength. With the increase of the content of cobalt, the fractured surface of ATC3 was characterized by a mixed mode of intergranular and transgranular fractures. The grain size became fine and homogeneous as shown in Fig. 2(b), and there were few pores left in the composite. According to the previous researches [14,15] cobalt was usually located at the TiC grain boundaries or the interfaces of $Al_2O_3$ and TiC, which can prevent or reduce clustering, merging and growing of particles in the sintering process. Additionally, the melting point of cobalt was much lower than the sintering temperature. Cobalt became fluid and could fill the pores among grains, thus the composite can possess a high relative density. However, with the increase of cobalt content the excessive cobalt cannot distribute uniformly in the composite. A mass of cobalt might form agglomeration at grain boundaries, which made the grain boundaries unclean and led to an inhomogeneous microstructure as shown in Fig. 2(c)–(d). The average grain size of ATC5 was much coarser than that of ATC3, which was harmful to the flexural strength but beneficial for improving the fracture toughness [16]. When the cobalt content was 8 vol%, there

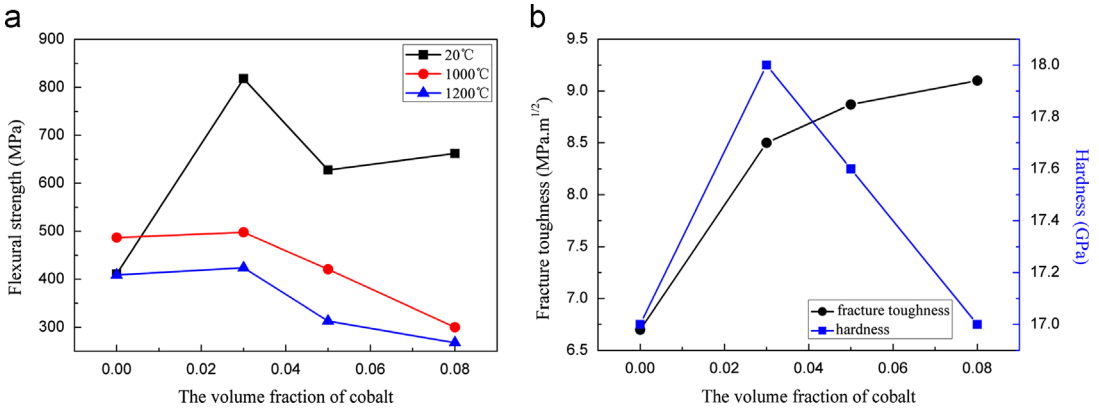


Fig. 1. Effects of cobalt content on (a) the ambient and high temperature flexural strength and (b) the ambient temperature fracture toughness and hardness.

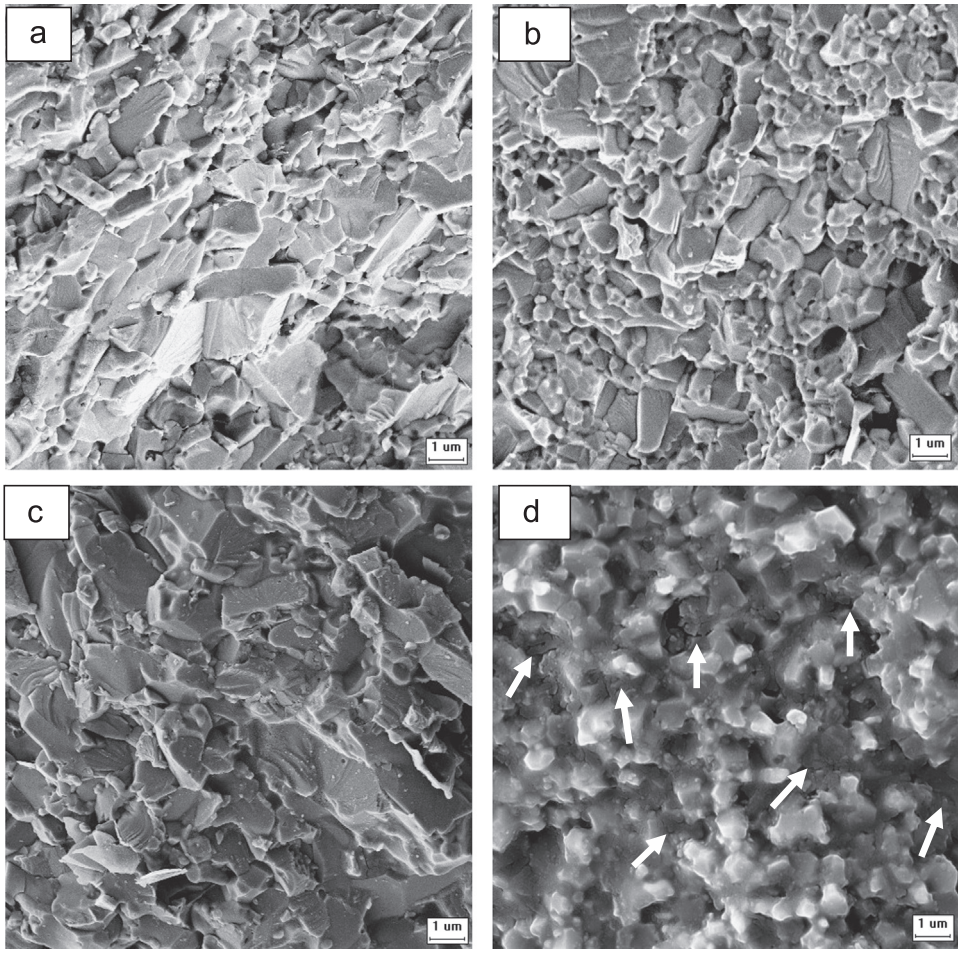


Fig. 2. SEM micrographs of fractured surfaces of the composites containing (a) 0, (b) 3, (c) 5 and (d) 8 vol% cobalt.

were some micro-cracks in the composite as indicated by arrows in Fig. 2(d). For $Al_2O_3$–TiC–Co composite, when cooled from 1650 °C to the room temperature, the distribution of residual stress can be calculated according to Ref. [17]. Large tensile stress distributed at the interface of Co and $Al_2O_3$, especially in the cobalt layer as shown in Fig. 3. The appearance of the micro-cracks could be associated with the tensile stress. These micro-cracks not only decreased the loading cross-sectional area but also caused the stress concentration, which resulted in the low flexural strength.

At high temperature, there was little difference in the flexural strength between ATC0 and ATC3, but the flexural strength had a significant degradation with the further increase of cobalt content. The high temperature strength of the composite containing the metal phase was much lower than the ambient temperature strength, however, there was little

difference between the ambient and high temperature strength of the composite without the metal phase. The stress–strain curves for the composites tested at 1000 °C are shown in Fig. 4. It can be seen that the fracture mode of all samples were of the brittle mode. The elastic modulus of the composites containing cobalt was lower than that of the composite without cobalt. It meant that the composites containing cobalt were much softer at high temperature.

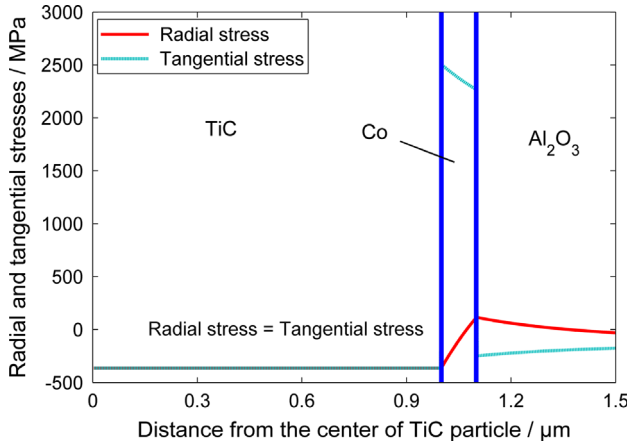


Fig. 3. The thermal residual stress distribution of $Al_2O_3$–TiC–Co composite.

Compared to the ambient temperature strength, the high temperature strength of the composites containing cobalt was much lower. It was well known that the degradation of strength of ceramics at high temperature always related to the softening of grain boundary, i.e., the change of fracture mode as a result of the grain boundary weakness, especially when low melting point phases existed at the grain boundaries [18–21]. As observed in ATC3 fractured at 800 °C (Fig. 5(a)), the grains with the cleavage steps (indicated by the circles) were much less than that of the sample fractured at 20 °C (Fig. 2(b)). It meant that the fracture mode at high temperature was mainly intergranular fracture. The change of the fracture character was the result of the intergranular boundary weakness at high temperature. The cobalt distributed at grain boundaries got soft at high temperature, leading to the poor interfacial bonding strength. It meant that cracks preferred to propagate intergranularly and less fracture energy was consumed.

An additional effect could be ascribed to the surface oxidation, as these tests were carried out in air. Kondo et al. reported that the fracture energy of $Si_3N_4$ ceramics tested in a nitrogen atmosphere at 1500 °C was larger than that tested in air [21]. In fact, after a thermal cycle at 1000 °C for about 1 h in air, the degradation of surface was evident as shown in Fig. 5(b). The effect of surface oxidation on strength degradation is analyzed in details in the following section.

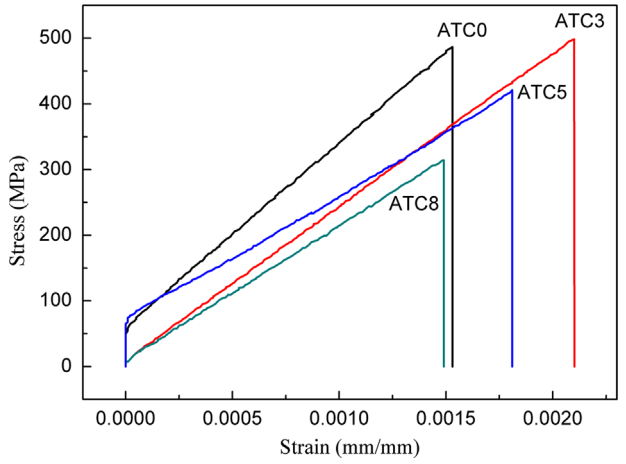


Fig. 4. The stress–strain curves for the composites tested at 1000 °C.

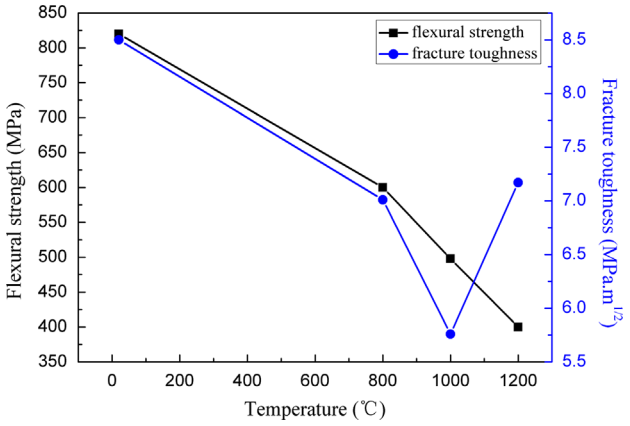


Fig. 6. The high temperature flexural strength and fracture toughness of ATC3.

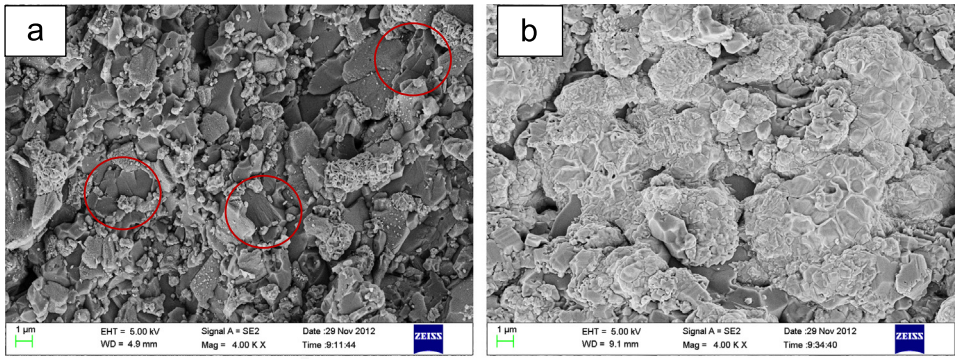


Fig. 5. SEM micrographs of the fractured surfaces of (a) ATC3 tested at 800 °C and (b) ATC5 oxidized at 1000 °C for about 1 h.

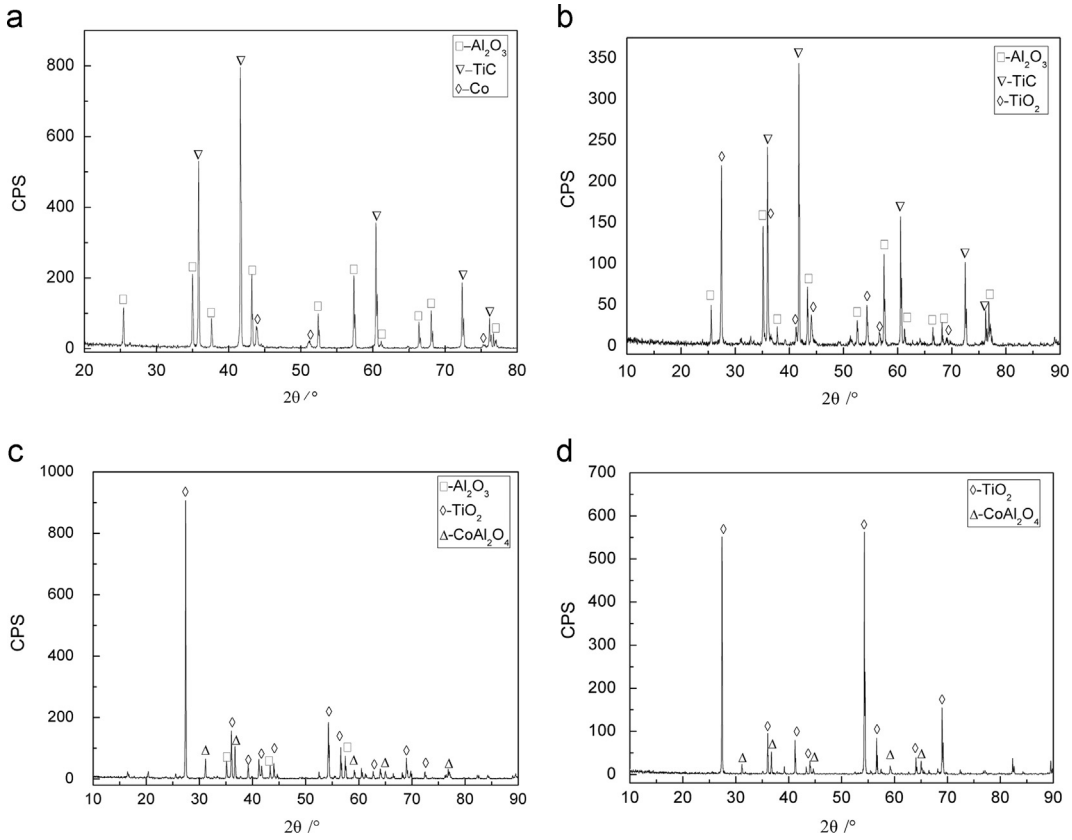


Fig. 7. The XRD patterns of ATC3 tested at (a) 20 °C, (b) 800 °C, (c) 1000 °C and (d) 1200 °C.

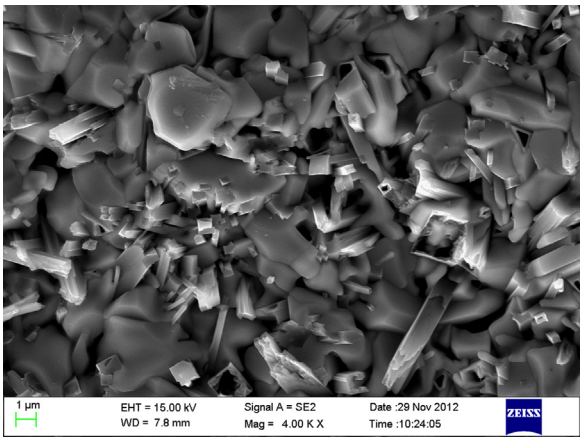


Fig. 8. The surface morphology of ATC3 tested at 1000 °C.

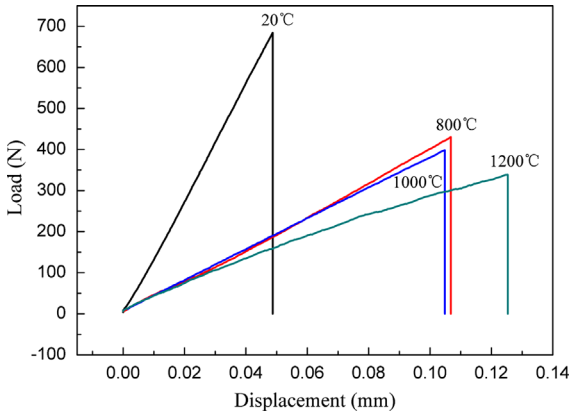


Fig. 9. The load–displacement curves for ATC3 tested at different temperatures.

### 3.2. High temperature flexural strength and fracture toughness

The flexural strength and fracture toughness of ATC3 versus the testing temperature are shown in Fig. 6. The flexural strength decreased as the temperature increased from 20 to 1200 °C, however, it still maintained a higher value (about 390 MPa) even at 1200 °C. The fracture toughness decreased as a function of the temperature up to 1000 °C but increased at 1200 °C.

The strength degradation was attributed to the oxidization of grains and grain boundaries. The XRD patterns of ATC3 tested at different temperatures are shown in Fig. 7. It can be seen from Fig. 7(a) that there was no chemical reaction among $Al_2O_3$, TiC and Co in the sintering process. TiC was oxidized to $TiO_2$ from 800 °C, and the oxidization became more severe as the temperature increased as indicated in Fig. 7(b)–(c). Shi et al. [22] studied the oxidation behavior of the $Al_2O_3$–TiC–Co composites and found that there was no oxidation reactions from 20 °C to 600 °C, and $Co_3O_4$ was detected both at 800 °C and 1000 °C. However, cobalt oxides in the present work were

not found. This was probably because $Co_3O_4$ existed below the thick $TiO_2$ layer, and this could not be detected by scanning the surface. Additionally, $Co_3O_4$ was decomposed into CoO at the temperature above 900 °C [23]. CoO could react with $Al_2O_3$ to form $CoAl_2O_4$ at high temperature [24]. Therefore, $CoAl_2O_4$ was found in the samples tested at 1000 °C and 1200 °C.

The surface morphology of ATC3 tested at 1000 °C was shown in Fig. 8. It can be seen that the grains and grain boundaries were destroyed badly, and some small holes appeared on the surface. For the present composite ceramics, oxygen primarily attacked the grain boundary phase, then the oxidation of $Al_2O_3$ and TiC grains occurred. The disappearance of the grain boundary phase and the formation of oxides contributed to inducing defects and cracks at the grain boundaries. The cracks progressively propagated toward the bulk material, inducing the dramatic strength degradation.

According to the load–displacement curves of ATC3 shown in Fig. 9, the sample tested at 20 °C showed the brittle fracture and little plastic deformation prior to failure. At 800 °C and 1000 °C, the fracture was brittle but the evidence of slight plastic deformation was observed prior to failure. At 1200 °C, the sample fractured with considerable plastic deformation. The elastic modulus decreased with the increase of temperature, which was another reason for the strength degradation.

Compared to Fig. 2(b), the grain morphology of the composite fractured at 1200 °C was irregular with quite a few folds as shown in Fig. 10, which was very different from that of the composite fractured at room temperature. This phenomenon should be attributed to the grain boundary sliding and grain plastic deformation at high temperature, as the composite presented considerable plastic deformation at 1200 °C. More fracture energy was dissipated through grain boundary sliding and grain plastic deformation, resulting in the enhanced fracture toughness at 1200 °C.

Grain boundary sliding in ceramics was always associated with grain boundary strength, impurities and segregation [20]. The probable reasons for the grain boundary sliding in the present composite at high temperature are as follows.

Firstly, the critical resolved shear stresses for basal and prism plane slips in a single α-alumina crystal decreased with the increase of the temperature [25]. It meant that the grain dislocations were easier to be generated at high temperature. Secondly, due to the mismatch of the thermal expansion coefficients between $Al_2O_3$ and TiC, a residual stress field around TiC particle was generated when cooled from 1650 °C to the room temperature. The average residual micro-stresses inside the TiC particle and the $Al_2O_3$ matrix were −370 MPa and 200 MPa, respectively according to the model established by Taya et al. [26]. Such residual stresses would relax when the testing temperature increased, i.e., the TiC grains could not contact with the adjacent $Al_2O_3$ grains as tightly as at room temperature. The release of the compressive stress across the TiC grain boundaries at high temperature can also accelerate their sliding mobility. Furthermore, cobalt distributed at the grain boundaries got soft at high temperature. The low viscosity metal phase contributed to the grain boundary sliding.

Stress concentration at grain boundaries was generated due to the grain boundary sliding. The stress concentration can make the grains get plastic deformation (Fig. 10), resulting in defects due to the dislocation pile-up [27]. It can also cause the micro-cracks at grain boundaries [28]. So, the sharp strength degradation at 1200 °C was mainly ascribed to the defects resulting from the grain boundary sliding.

## 4. Conclusions

(1) The ambient temperature mechanical properties and high temperature flexural strength of the composite ceramic tool materials were influenced greatly by the content of cobalt. Bits of cobalt could dramatically improve the ambient temperature mechanical properties, and had little disadvantage to the high temperature strength. However, excess cobalt made the high temperature strength decrease because cobalt was easier to be oxidized and get soft at high temperature in air.

(2) The elastic modulus of the composite decreased with the increase of temperature. The fracture toughness of ATC3 decreased as the temperature increased from 20 to 1000 °C, but slightly increased at 1200 °C. The flexural strength of ATC3 decreased with the increase of temperature, but it can still keep a high strength even at 1200 °C. These characters of the present composite ceramic make it feasible to be used as a cutting tool in the high speed machining.

(3) The composite ceramic tool material presented plastic deformation prior to failure at high temperature, especially

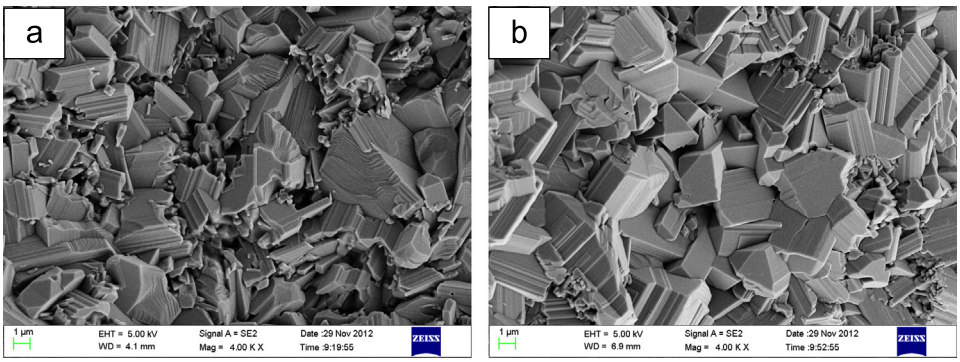


Fig. 10. SEM micrographs of fractured surfaces of ATC3 after (a) the three-point bending test at 1200 °C and (b) the SENB test at 1200 °C.

at 1200 °C. More fracture energy was dissipated through grain plastic deformation, resulting in a slight increase of fracture toughness at 1200 °C. The reasons for the strength degradation at high temperature were the change of the fracture mode due to the softening of cobalt distributed at the grain boundaries, the grain and grain boundary oxidation, the decrease of elastic modulus and the grain boundary sliding.

## Acknowledgments

The work is supported by the National Natural Science Foundation of China (50975161 and 51005136), and the Key Special Project of Numerical Control Machine Tool (2012ZX04003-051).

## References

[1] X. Ai, H. Xiao, Machining with the Ceramic Cutting Tools, China Machine Press, Beijing, 1988 (in chinese).
[2] Y.L. Dong, F.M. Xu, X.L. Shi, Fabrication and mechanical properties of nano-/micro-sized $Al_2O_3$/SiC composites, Materials Science and Engineering: A 504 (2009) 49–54.
[3] N. Liu, Y.D. Xu, H. Li, Effect of nano–micro TiN addition on the microstructure and mechanical properties of TiC based cermets, Journal of the European Ceramic Society 22 (2002) 2409–2414.
[4] J. Zhao, X.L. Yuan, Y.H. Zhou, Processing and characterization of an $Al_2O_3$/WC/TiC micro–nano-composite ceramic tool material, Materials Science and Engineering: A 527 (2010) 1844–1849.
[5] X.Y. Teng, H.L. Liu, C.Z. Huang, Effect of $Al_2O_3$ particle size on the mechanical properties of alumina-based ceramics, Materials Science and Engineering: A 452 (2007) 545–551.
[6] N. Liu, M. Shi, Y.D. Xu, Effect of starting powders size on the $Al_2O_3$–TiC composites, International Journal of Refractory Metals and Hard Materials 22 (2004) 265–269.
[7] B. Zou, C.Z. Huang, H.L. Liu, Study of the mechanical properties, toughening and strengthening mechanisms of $Si_3N_4$/$Si_3N_{4w}$/TiN nano-composite ceramic tool materials, Acta Materialia 55 (2007) 4193–4202.
[8] Z.M. Zhao, L. Zhang, J. Zheng, Microstructures and mechanical properties of $Al_2O_3$/$ZrO_2$ composite produced by combustion synthesis, Scripta Materialia 53 (2005) 995–1000.
[9] W. Acchar, Y.B.F. Silva, C.A. Cairo, Mechanical properties of hot-pressed $ZrO_2$ reinforced with (W, Ti) C and $Al_2O_3$ additions, Materials Science and Engineering: A 527 (2010) 480–484.
[10] L.S. Sigl, P.A. Mataga, B.J. Dalgleish, On the toughness of brittle materials reinforced with a ductile phase, Acta Metallurgica 36 (1988) 945–953.
[11] Z.B. Yin, C.Z. Huang, B. Zou, Preparation and characterization of $Al_2O_3$/TiC micro–nano-composite cetamic tool materials, Ceramics International 39 (2013) 4253–4262.
[12] C.Z. Huang, X. Ai, The characteristics of the cutting force and temperature when machining nickel-base alloys, Tool Engineering 29 (1995) 35–37.
[13] Y.W. Bao, Y.M. Wang, Z.Z. Jin, Creep and stress ageing of $Al_2O_3$/SiC multiphase ceramics at high temperature, Journal of the Chinese Ceramic Society 28 (2000) 348–351.
[14] D.S. Mao, X.H. Liu, J. Li, A fine cobalt-toughened $Al_2O_3$–TiC ceramic and its wear resistance, Journal of Materials Science 33 (1998) 5677–5682.
[15] J. Li, J.L. Sun, L.P. Huang, Effects of ductile cobalt on fracture behavior of $Al_2O_3$–TiC ceramic, Materials Science and Engineering: A 323 (2002) 17–20.
[16] J.H. Gong, H.Z. Miao, Z. Zhao, Effect of TiC particle size on the toughness characteristics of $Al_2O_3$–TiC composites, Materials Letters 49 (2001) 235–238.
[17] G.F. Mi, H.W. Wang, X.Y. Liu, Analysis of thermal stress in the TiC/$Ti_3AlC$/$Ti_3Al$ three-phase composites, Rare Metal Materials and Engineering 36 (2007) 172–177.
[18] Y.W. Kim, Y.S. Chun, T. Nishimura, High-temperature strength of silicon carbide ceramics sintered with rare-earth oxide and aluminum nitride, Acta Materialia 55 (2007) 727–736.
[19] M. Boniecki, Z. Librant, A. Wajler, Fracture toughness, strength and creep of transparent ceramics at high temperature, Ceramics International 38 (2012) 4517–4524.
[20] J. Zou, G.J. Zhang, C.F. Hu, High-temperature bending strength, internal friction and stiffness of $ZrB_2$–20 vol% SiC ceramics, Journal of the European Ceramic Society 32 (2012) 2519–2527.
[21] N. Kondo, Y. Suzuki, T. Miyajima, High-temperature mechanical properties of sinter-forged silicon nitride with ytterbia additive, Journal of the European Ceramic Society 23 (2003) 809–815.
[22] R.X. Shi, J. Ding, Y.Q. Cao, Oxidation behavior and kinetics of $Al_2O_3$–TiC–Co composites, International Journal of Refractory Metals and Hard Materials 36 (2013) 130–135.
[23] Q.S. Zhang, Y. Takeda, Mechanism of infiltrated cobalt oxide effect on LSM–YSZ cathode performance, Journal of the Chinese Rare Earth Society 25 (2007) 183–189.
[24] N.W. Zhang, C.J. Huang, F.P. Kuang, Effect of a Mg promoter on the structure and catalytic performance of a Co/Mg/HZSM-5 catalyst for the partial oxidation of methane to syngas, Acta Physico-Chimca Sinica 24 (2008) 2165–2171.
[25] S.M. Choi, H. Awaji, Nanocomposites—a new material design concept, Science and Technology of Advanced Materials 6 (2005) 2–10.
[26] M. Taya, S. Hayashi, A.S. Kobayashi, Toughening of a particulate-reinforced ceramic–matrix composite by thermal residual stress, Journal of the American Ceramic Society 73 (1990) 1382–1391.
[27] C. Baudín, R. Martínez, P. Pena, High-temperature mechanical behavior of stoichiometric magnesium spinel, Journal of the American Ceramic Society 78 (1995) 1857–1862.
[28] T. Ohji, Y. Yamauchi, Diffusional crack growth and creep rupture of silicon carbide doped with alumina, Journal of the American Ceramic Society 77 (1994) 678–682.